Deposited via The University of Sheffield.

White Rose Research Online URL for this paper:
https://eprints.whiterose.ac.uk/id/eprint/238783/

Version: Published Version

Article:

Closing the denitrification gap: applying the ^{15}N gas flux method with an artificial atmosphere in conventional and regenerative agriculture

Gianni Micucci[1]*, Fotis Sgouridis[2], Jonathan Leake[3] and Sami Ullah[1,4]*

[1]School of Geography, Earth and Environmental Sciences, University of Birmingham, Birmingham, United Kingdom, [2]School of Geographical Sciences, University of Bristol, Bristol, United Kingdom, [3]Plants, Photosynthesis and Soil, School of Biosciences, University of Sheffield, Sheffield, United Kingdom, [4]Birmingham Institute of Forest Research, University of Birmingham, Birmingham, United Kingdom

Introduction: Denitrification is an elusive process that remains notoriously difficult to measure under field conditions, yet it plays a crucial role as the only natural terrestrial sink for reactive nitrogen, especially in agricultural systems where large amounts of fertilizer are applied. Direct measurements of N_2 fluxes over extended periods remain rare in the literature due to technical challenges.

Methods: In this study, we quantified and characterized denitrification emissions under two contrasting land-use practices—conventional and regenerative (unfertilized) agriculture—using a recently developed custom method combining a ^{15}N isotopic tracer with an artificial atmosphere (improved ^{15}N Gas Flux method). We conducted nine field campaigns over one year to (i) assess method applicability, (ii) derive a first annual estimate of denitrification, (iii) understand controls on denitrification dynamics, and (iv) trace denitrification-driven losses of applied synthetic nitrogen fertilizer in conventional agriculture.

Results: Our method successfully detected denitrified N_2 fluxes in 90% of measurements and yielded annual budgets of 22.12 and 2.41 kg N ha^{-1} yr^{-1} in the conventional and regenerative fields, respectively. Soil moisture and nitrate availability (particularly under fertilized conditions) were the main controls on the denitrification product ratio ($N_2O/(N_2O + N_2)$). We estimated that 11% of applied fertilizer nitrogen was lost via denitrification in the conventional field, with 7.3% of this loss emitted as N_2O rather than N_2.

Discussion: These results underscore the role of fertilization management in shaping denitrification dynamics and its potential to act as a sink for reactive nitrogen, while modulating N_2O emissions.

KEYWORDS

15N gas flux method, denitrification, nitrogen cycling, nitrous oxide emission, regenerative agriculture

1 Introduction

Regenerative agriculture aims to restore degraded soil health, prevent the loss of arable land, and reduce overall agriculture's contribution to global warming. It revolves around five principles: minimum mechanical soil disturbance (i.e., no tillage), permanent soil organic cover, species diversification, keeping living roots in the soil and integrating animals (Miller-Klugesherz and Sanderson, 2023). A typical practice of regenerative agriculture is the "leys", introduced during the second agricultural revolution in Europe during the 18th century as part of arable rotations (Overton, 1996). It consists of converting a farmland into a temporary pasture (up to 5 years) to restore soil health and break pest cycles. In particular, "herbal leys" have been promoted for over a century in temperate regions (Jordon et al., 2022) and consist of complex mixtures of legumes, perennial forbs, herbs and grasses up to 100 species mix. The presence of livestock through rotational grazing enhances nutrient cycling, while the symbiotic association between legumes and nitrogen-fixing bacteria enable the leys to naturally fertilize soils via biological nitrogen fixation (BNF). It is estimated that BNF can fix approximately 200 million tonnes of nitrogen annually (Biswas and Gresshoff, 2014) and could therefore be a reliable alternative to synthetic nitrogen fertilizer. Such land management practices are expected to influence both the internal nitrogen (N) cycling and the overall N economy of farmlands, which are among the main contributors to the massive transgression of the planetary boundary for reactive nitrogen—currently exceeded by more than a factor of three (Rockström et al., 2023). Sustainable N management is thus critical to ensure future food security and environmental protection, but remains challenging to implement, partly because of the limited ability to quantify key nitrogen loss pathways under field conditions.

Among these pathways, denitrification remains the most uncertain and represents one of the primary sources of nitrous oxide emissions in agricultural ecosystems (Bremner, 1997). Denitrification is the sequential microbial dissimilatory respiration process which converts soil nitrate (NO_3^-) into gaseous dinitrogen (N_2); with the intermediates of nitrite (NO_2^-), nitric oxide (NO) and nitrous oxide (N_2O). When incomplete, it leads to the emission of N_2O, a greenhouse gas with a 273 times greater radiative forcing than CO_2 over 100 years (IPCC, 2023) and which is also involved in the depletion of the ozone layer (Ravishankara et al., 2009). On the other hand, the full process sequence is the main natural terrestrial sink for N_2O emissions (Conthe et al., 2019). A wide range of bacterial groups are capable of performing denitrification: *Bacillus, Enterobacter, Micrococcus, Pseudomonas, Spirillum, Proteus, Aerobacter* and *Flavobacterium* (Meng et al., 2014). Some fungi also possess the capability for denitrification although in general, they lack the nitrous oxide reductase enzyme necessary to reduce N_2O into N_2 (Matsuoka et al., 2017). For this reason, it is assumed these fungi contribute mostly to N_2O emissions (Laughlin et al., 2002). Denitrification has been shown to be regulated by oxygen levels (with low oxygen conditions, especially under elevated moisture, promoting the process), soil pH, nitrate availability, and supply of carbon substrates (Seitzinger et al., 2006). However, many uncertainties remain around this process (Groffman et al., 2006; Almaraz et al., 2020); including its potential magnitude and efficiency as a nitrous oxide sink. This efficiency is measured through the denitrification product ratio, defined as $N_2O/(N_2O + N_2)$, which represents the proportion of denitrification product emitted as N_2O.

Furthermore, denitrification dynamics are poorly constrained under intensive agriculture, where 120 million tonnes of nitrogen (N) fertilizer are applied annually worldwide (FAO - Food and Agriculture Organization of the United Nations, 2017), leading to increased denitrification emissions (Hofstra and Bouwman, 2005; Munch and Velthof, 2007). This lack of constraint is due to the high spatial and temporal variability of denitrification as well as the intrinsic difficulties linked to its measurement, i.e., the sensitivity required to detect small soil N_2 fluxes against the high atmospheric background (78%; Groffman et al., 2006; Micucci et al., 2023). Due to these technical challenges, denitrification losses are often inferred from the unexplained difference between N inputs and outputs in agricultural N budgets (Soana et al., 2022). However, this approach results in uncertainties regarding the pathways of N losses from unused fertilizer, which are estimated to represent half of the applied rate (Lassaletta et al., 2014). To address this issue, new methodologies have recently been developed, combining the use of ^{15}N isotopes (^{15}N Gas flux method "^{15}NGF"; Micucci et al., 2023) with an artificial atmosphere depleted in N_2 (Well et al., 2019b; Friedl et al., 2020; Wang et al., 2020; Bizimana et al., 2022) and have enabled tracing *in situ* dynamics of denitrification over a growing season for the first time (Eckei et al., 2024). However, denitrification dynamics have not yet been constrained over an annual cycle, to characterize temporal patterns during but also outside of the fertilization period. We have recently developed our own method to incubate soil cores for denitrification measurements under *in situ* field conditions (improved ^{15}N Gas Flux method, Micucci et al., 2024), using $^{15}N-NO_3$ tracer addition and an artificial atmosphere depleted in N_2 (5%). This method enables N_2 detection with high sensitivity (480 ppb), and it is applied here for the first time to quantify field-scale denitrification rates.

In this study, we aimed to characterize denitrification in two key land uses: conventional and regenerative agricultures over a full annual cycle (March 2022 to February 2023). Our research objectives were to:

1. Validate the applicability of our updated isotope-based denitrification method under field conditions and over an extended monitoring campaign, by (a) evaluating potential stimulation effects following $^{15}NO_3^-$ tracer application, and (b) determining the most appropriate approach to upscale flux measurements from soil cores to the field scale.
2. Derive a denitrification emission factor (D_{EF}) representing the proportion of applied synthetic N fertilizer lost via denitrification in conventional agriculture.
3. Derive a first budget of annual denitrification losses using our nine field measurements and establish field-scale denitrification product ratios in both fields.
4. Study the environmental controls on denitrification.
5. Characterize the temporal variations of denitrification.

2 Materials and methods

2.1 Study sites and experimental layout

This study took place at FarmED, near Shipton-under Wychwood UK (51.869981,-1.581136, https://www.farm-ed.co.uk/).

FarmED is an experimental agricultural station founded in 2018, consisting of strips of the same soil type under rotational herbal ley management (1–5 years). Prior to this layout, the soil (cambisol with an oolitic limestone bedrock) had been conventionally managed during 30 years for wheat and barley production. One experimental strip has been conserved under this conventional management (referred to as the arable strip). It includes the production of wheat and barley, minimum tillage and application of fertilizer, pesticides and herbicides. The herbal ley strips were all sown with the same mix, which includes white and red clovers (*Trifolium repens* and *Trifolium pratense* respectively), timothy (*Phleum pratense*), chicory (*Cichorium intybus*), lucerne (*Medicago sativa*) or sainfoin (*Onobrychis viciifolia*) among others (see Supplementary Table S1). For the present work, the 4-year-old herbal ley strip was studied and compared to the arable strip for a full year.

During our field campaign (April 2022–May 2023), the arable strip was sown with winter wheat in September 2021, which was harvested in August 2022, resown in October 2022 before being harvested again in August 2023. The herbal ley was mob-grazed by cows and sheep in July 2022 and April 2023. Synthetic liquid fertilizer was applied in the arable field with a rate of 179.5 kg N ha^{-1} in three applications (Supplementary Table S2).

In this study, we selected eight locations in parallel within both fields (Supplementary Figure S1), where denitrification emissions from soil cores were measured (9 measurements during the study year) using our newly developed method (Micucci et al., 2024), field fluxes of N_2O and CO_2 were measured using conventional static chambers, and soil was sampled and brought back to the laboratory for quantification of N nutrients (nitrate and ammonium), dissolved organic carbon (DOC) and soil moisture.

2.2 Soil characterization

During each measurement campaign, three soil samples were taken near core sampling locations (*n* = 8 per field) using a hand auger to a depth of 15 cm. These samples were then mixed to generate one composite sample per chamber location. After collection, they were transported to the laboratory, sieved to <2 mm, and stored at 4 °C in a refrigerator until further processing.

For mineral nitrogen analysis, 5 g of soil were extracted using a 0.5 M potassium sulfate (K_2SO_4) solution at a 1:8 ratio. The extraction mixture was shaken for 2 h at 200 rpm, followed by centrifugation at 3,000 rpm for 5 min. The supernatant was subsequently filtered through a 0.45 μm syringe filter and analyzed using a San++ continuous flow analyzer (Skalar, Breda, Netherlands). Nitrate (NO_3^-) concentrations were determined via cadmium reduction, while ammonium (NH_4^+) was measured using the modified Berthelot reaction. Detection limits were 0.02 mg N L^{-1} for NO_3^- and 0.05 mg N L^{-1} for NH_4^+, with blank correction applied. For the quantification of dissolved organic carbon (DOC), 5 g of soil were extracted using 40 mL of deionized water, then shaken at 200 rpm on an orbital shaker for 2 h. The extracts were subsequently filtered through Whatman No. 42 paper (GE Healthcare). Filtrate analysis was performed using a Shimadzu TOC-L analyzer (Japan), with a detection limit of 1 ppm for DOC. Moisture content was measured gravimetrically based on mass loss after drying at 105 °C

for 24 h and is expressed relative to dry mass. Water-filled pore space (WFPS) was calculated using bulk density and assuming a soil particle density of 2.65 g cm^{-3}. Other soil characteristics (such as texture, pH, organic matter content, etc.) were measured once at the start of the study and are presented in Supplementary Table S3.

2.3 Measurement of denitrification

We measured denitrification *in situ* using our newly developed method (Micucci et al., 2024), which combines the ^{15}NGF with an artificial atmosphere depleted in N_2. Briefly, 10 cm-high intact soil cores (n = 8 per land-use type; 16 cores per month in total) were sampled inside 15 cm-long plastic liners (4.6 cm ID) and left to pre-incubate overnight under environmental conditions. The next day, ^{15}N-NO_3^- tracer solutions were prepared by dilution of K-^{15}NO$_3$ (98 at% ^{15}N, Merck) and applied to reach a 50% ^{15}N enrichment of the soil denitrifying pool (based on measured nitrate levels) and to induce an increase in gravimetric soil moisture <5% via 40 injections (at 0, 2.5, 5 and 10 cm depth). The liners were subsequently capped with gas tight lids with butyl rubber septa and flushed with a gas mixture containing 5% N_2, 20% O_2, 75% He and 0.11 ppm of N_2O (Supplementary Figure S1), and left to incubate in freshly dug holes in the soil under environmental conditions. Gas sampling occurred at times 0, 2 and 4 h where 15 mL of the liner's headspace were sampled and transferred to pre-evacuated 12 mL Exetainer vials (Labco, UK). To equilibrate the loss of pressure, 15 mL of the artificial gas mixture were transferred back to the liners' headspace. Errors resulting from this sampling procedure and diffusive fluxes due to incomplete liner sealing were corrected as detailed in Micucci et al. (2024). Upon return to the laboratory, 1 mL of the gas samples was analysed on an Agilent 7890A gas chromatograph to determine N_2O and CO_2 concentrations, with repeatability (1σ) of 3 ppb and 11 ppm, respectively. The remaining 14 mL of the samples were analysed over a continuous flow IRMS (Elementar Isoprime PrecisION; Elementar Analysensysteme GmbH, Hanau, Germany) for the determination of ratios R29 ($^{29}N_2$/$^{28}N_2$) and R30 ($^{30}N_2$/$^{28}N_2$) for N_2 as well as ratios R45 ($^{45}N_2O$/$^{44}N_2O$) and R46 ($^{46}N_2O$/$^{44}N_2O$) for N_2O. The repeatability (1σ) for these measurements were (1.5 × 10^{-6}) for R29, (9.3 × 10^{-6}) for R30, (3.1 × 10^{-5}) for R45 and (8.2 × 10^{-5}) for R46. The full description of these analyses can be found in Section 2 of the Supplementary File. Denitrified N_2 and N_2O fluxes were calculated using the approach described in Micucci et al. (2024).

From the liner measurements, we calculated two denitrification parameters, the source partitioning coefficient (SPC) and the macroscopic product ratio (R_{N2O}, see Micucci et al., 2025) defined as per Equations 1, 2:

$$SPC = \frac{f_{N2O\,denitrified}}{f_{N2O\,total}} \qquad (1)$$

$$R_{N2O} = \frac{f_{N2O\,denitrified}}{f_{N2O\,denitrified} + f_{N2\,denitrified}} \qquad (2)$$

Where f is a flux of nitrogen (either as N-N_2O or N-N_2; in kg N ha^{-1} month^{-1}). The SPC represents the part of soil N_2O emissions attributable to denitrification while the R_{N2O} represents the proportion of denitrification product emitted as N_2O rather than N_2.

2.4 Total N_2O and CO_2 flux measurement using static chambers

Two weeks before the measurement campaign of April 2022, eight collars (20 cm OD, 15 cm height) were inserted 10 cm deep into the soil for installing conventional static chambers (20 cm OD, 20 cm total height) in both the herbal ley and the arable field (Supplementary Figure S1). Because of the distance between chambers and the fact that the soil core incubation was running at the same time, the sampling of the chambers' headspace occurred every hour for 2 h. Since this does not respect the criterion of chamber height to deployment time ratio ≥40 cm h^{-1} recommended by Zaman et al. (2021), we corrected for diffusion issues using the HMR model (Pedersen et al., 2010), with the associated R script (R Core Team 2023) from CRAN (Comprehensive R Archive Network). To illustrate the magnitude of the diffusion correction, in May 2022, 14 out of 16 chambers required this correction, leading to an average 47% increase in N_2O fluxes. This is consistent with the results of Anthony et al. (1995) and Pedersen et al. (2010), who reported values of 54% and 52% respectively. Gas samples were collected and analysed using the same approach as for the cores, but without the IRMS analysis.

2.5 Deriving field-scale denitrification budgets

While our nine field campaigns represent a limited temporal resolution at the annual scale, they still allow us to derive a first-order denitrification budget and estimate field-scale denitrification product ratios. Chamber and core measurements both have strengths and limitations. Open-bottom static chamber measurements do not require soil disturbance (after initial insertion of the chamber collar) and capture the integrated soil profile emissions at the study location. They are however sensitive to downward or lateral diffusive losses, especially for prolonged measurement times (Hutchinson and Mosier, 1981), which can lead to underestimations of total denitrification fluxes by up to 37% (Well et al., 2019b). These diffusive exchanges with the ambient air also prevent the use of an artificial atmosphere (Micucci et al., 2024). On the other hand, the seal of the liners enables them to retain the artificial atmosphere for prolonged periods of time, allowing for N_2 detection, and their bottom-closed structure prevents diffusive losses. However, the magnitude of flux measured through these liners is probably not representative of field rates, given the small height (10 cm) and surface area (ID 5 cm) of the cores. Nonetheless, since most of the denitrification activity occurs in that zone (more generally in the tillage zone; Groffman et al., 2009; Well et al., 2019a), we hypothesized that the dynamics of denitrification and in particular the SPC and R_{N2O} coefficients measured through these cores would be representative of field dynamics. Combining these coefficients with the N_2O fluxes measured from static chambers we can derive an alternative denitrification budget, as follows:

$$f_{N2O\,denitrified} = SPC \times f_{N2O\,chamber} \qquad (3)$$

$$f_{N2} = f_{N2O\,denitrified} \times \frac{(1 - R_{N2O})}{R_{N2O}} \qquad (4)$$

Where $f_{N2O\,chamber}$ is the flux of N-N_2O derived from the static chamber measurements. Given that the soil beneath the flux

chambers remained isolated throughout the entire campaign (due to the collars inserted 10 cm deep, see Section 2.4), while new soil cores had to be sampled near the chamber locations every month, and given that denitrification exhibits high spatial variability at the micro-scale, monthly averages were used for chamber-based N_2O flux magnitudes as well as denitrification parameters. The propagation of error was determined as per Equations 5, 6:

$$SE\left[f_{N2O\,denitrified}\right] = \sqrt{\frac{\left(SPC \times SE\left[f_{N2O\,chamber}\right]\right)^2}{+\left(SE[SPC] \times f_{N2O\,chamber}\right)^2}} \qquad (5)$$

$$SE[f_{N2}] = \sqrt{\frac{\left(SE\left[f_{N2O\,denitrified}\right] \times \frac{(1-PR)}{PR}\right)^2}{+\left(SE[PR] \times \frac{f_{N2O\,denitrified}}{PR^2}\right)^2}} \qquad (6)$$

Where SE is the standard error.

2.6 Statistics and calculations

To take into account our experimental design (measurements repeated in time and space), we used linear mixed models with the lme4 package of R (R Core Team 2023). The unique combination of "Month" and "Land Use Type" was used as a random factor named "unique_sample".

Models were validated by assessing the normality and homoscedasticity of residuals, and the best-fitting model was selected using the Akaike Information Criterion (AIC). Type III ANOVA, using the Satterthwaite method was performed to assess the effect and significance of the different predictors. To characterize the temporal patterns of the study variables, we used linear interpolation between monthly means; yearly fluxes were derived using the trapezoidal rule. All results are given ±standard error.

3 Results

3.1 *In situ* denitrification and CO_2 measurements

The evolution of total N_2O emissions (Figure 1a) and denitrified N_2O emissions (Figure 1c) measured with the liners showed a clear peak in May 2022 in the arable field (respectively 0.84 ± 0.16 and 0.32 ± 0.15 kg N ha^{-1} month^{-1}), during the fertilization period (March to May 2023). At the same time, N_2 emissions were relatively low 0.92 ± 0.31 kg N ha^{-1} month^{-1} (Figure 1d), which resulted in the highest product ratio recorded during our monitoring period, with a value of 32.0% ± 7.8%. Interestingly, in the prior month (April 2022), the opposite trend is observed, with a high peak of N_2 production at 4.13 ± 0.81 kg N ha^{-1} month^{-1} and modest emissions of denitrified N_2O at 0.09 ± 0.02 kg N ha^{-1} month^{-1}, resulting in a product ratio of 3.7% ± 1.3%. Other than that, emissions were relatively stable with denitrified N_2 emissions around 1 kg N ha^{-1} month^{-1} in both fields and denitrified N_2O emissions around 0.1 kg N ha^{-1} month^{-1}. There was a second peak of N_2O emissions in October, observed both in the liners (total and
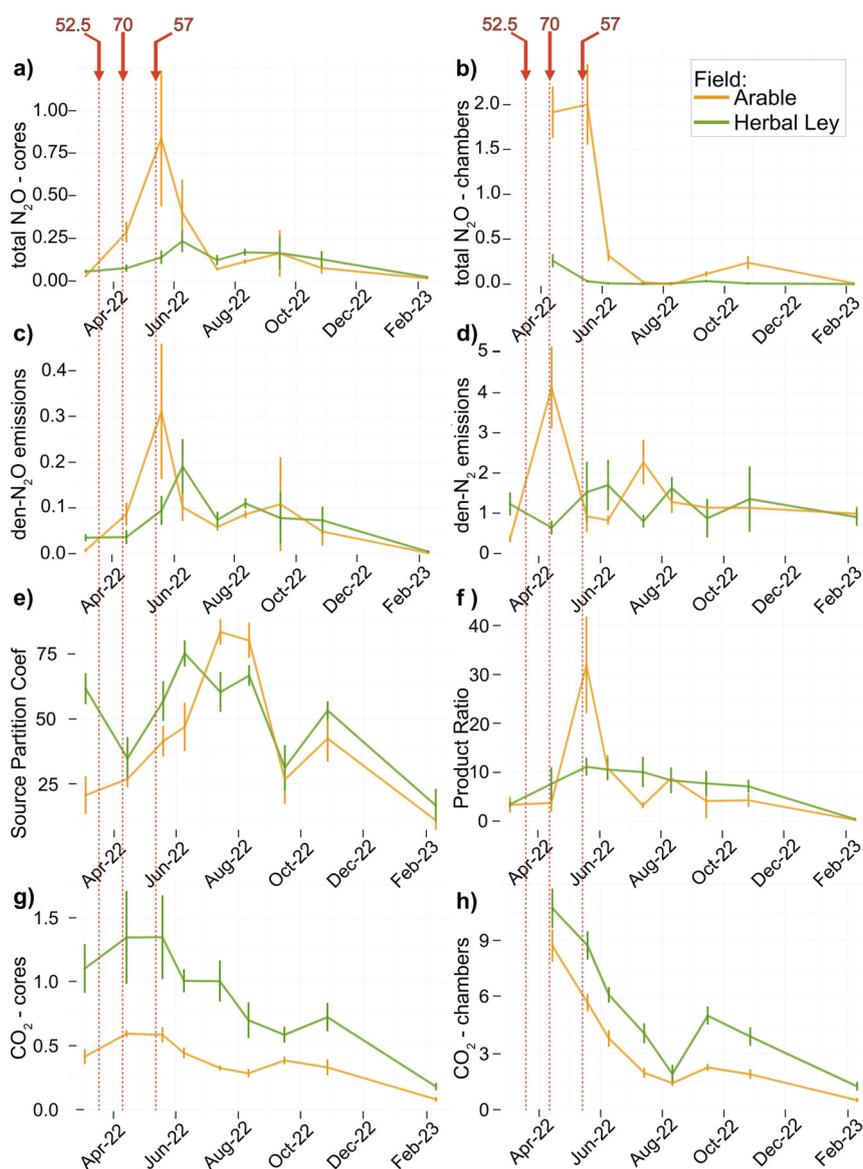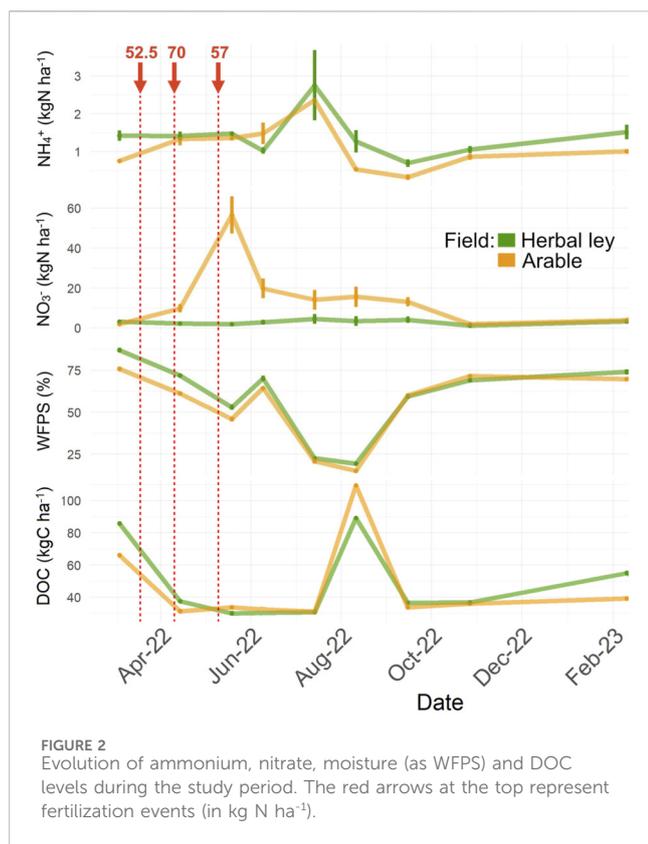
FIGURE 1
Total N$_2$O emissions from soil cores **(a)** and chambers **(b)**, denitrified N$_2$O **(c)** and N$_2$ **(d)** emissions measured from the soil cores, source partitioning coefficient **(e)**, denitrification product ratio **(f)**, CO$_2$ emissions from cores **(g)** and from chambers **(h)**. N$_2$ and N$_2$O fluxes are expressed in kg N ha^{-1} month^{-1}, CO$_2$ fluxes are expressed in t ha^{-1} month^{-1} and the two denitrification coefficients are expressed in %. The red arrows represent the fertilizer application (total N inputs in kg ha^{-1}). The error bars represent the standard errors.

denitrified) and the chambers. The SPC coefficients for both fields were characterized by an almost Gaussian evolution between the months of March and September (Figure 1e), with some anomalies for the herbal ley, having a peak at 62% ± 10% in March and another peak in July with 75% ± 12%. Similar to N$_2$O emissions, a second smaller peak event was observed around the month of October for both fields. On the other hand, the denitrification product ratios (Figure 1f) were mostly under 15%, at the exception of the month of May 2022 as mentioned previously. We can note that our newly developed method was successful at measuring denitrified N$_2$ emissions 90% of the time (n$_{total}$ = 144).

The total N$_2$O emissions from cores and chambers were in the same order of magnitude (~1 kg N ha^{-1} month^{-1} Figures 1a,b). However, the emissions from the herbal ley tended to be higher in

the liners, especially from May 2022 onwards, where they were on average 0.12 kg N ha^{-1} month^{-1} compared to 0.02 kg N ha^{-1} month^{-1} in the chambers. A peak of emissions (0.26 kg N ha^{-1} month^{-1}) was observed in the chambers in April 2022 but not in the liners. The same thing is observed in the arable field, where peak of almost 2 kg N ha^{-1} month^{-1} is observed in the chambers in April 2022 but not in the liners.

Finally, the fluxes of CO$_2$ followed the same pattern whether they were measured with chambers or liners. They were at an all-time high in April 2022 and decreased gradually until August 2022 before a local spike in October 2022 and decreasing to reach all time low levels in February 2023. However, the fluxes measured through the chambers were about 6 times higher than in the liners.

FIGURE 2
Evolution of ammonium, nitrate, moisture (as WFPS) and DOC levels during the study period. The red arrows at the top represent fertilization events (in kg N ha⁻¹).

3.2 Ammonium, nitrate, moisture and DOC content

The ammonium content of the two land uses stayed relatively constant (below 3 kg N ha⁻¹; Figure 2) despite fertilizer application, which contained approximately 75% of ammonia and urea (Supplementary Table S2). On the other hand, fertilizer application in 2022 resulted in a clear increase of the observed nitrate concentration in the arable field (Figure 2). The three applications of fertilizer in 2022 (~41.5 kg N ha⁻¹ of N-NO$_3$, Supplementary Table S2) led to significantly elevated nitrate levels, reaching 56.8 ± 9.8 kg N ha⁻¹ in May. Fertilizer-derived nitrate accumulated and persisted in the soil until October, at which point the nitrate levels reached their pre-fertilization levels (~2 kg N ha⁻¹). On the other hand, the herbal ley had low and constant amounts of available nitrate (<5 kg N ha⁻¹), except for a moderate increase from July to September 2022.

For both fields, moisture decreased from March 2022 (WFPS ~75%) to August 2022 (~20%) at the exception of June 2022, which saw a local maximum peak (70%) due to extremely wet conditions (Figure 2). From there, the moisture levels rose again up to the end of October 2022, where they stabilized until the end of the field campaign in February 2023.

On average, the herbal ley retained more moisture than the arable field. Finally, DOC levels in both fields showed peak events in August 2022 (~100 kgC ha⁻¹) which coincide with the grazing period in the herbal ley and the presence of crop residues following harvesting in the arable field. There were also peaks of DOC levels in April 2022 and 2023 (~70 kgC ha⁻¹, except in the herbal ley in 2023) aligning with the early spring surge in plant and

microbial activity. Otherwise, the levels remained relatively steady (between 25 and 50 kgC ha⁻¹).

3.3 Environmental controls on denitrification

To analyse the dependence of denitrification with environmental variables, we performed linear mixed model analyses as described in Section 2.6. Our four dependent variables were the flux of denitrified N$_2$O, flux of denitrified N$_2$, source partitioning coefficient as well as product ratio. Since none of these variables followed a normal distribution, we had to use non-linear transformations. The fluxes of denitrified N$_2$O and N$_2$ were log-transformed (Supplementary Figure S2). The SPC and R$_{N2O}$ parameters varied between 0 and one and therefore could not be long transformed. A Box-Cox test determined that a square root transformation was the most appropriate (Supplementary Figure S3), resulting in these ratios approximating a normal distribution (Supplementary Figure S4). While other studies have used a Beta transformation (e.g., Eckei et al., 2024), our data were more normally distributed using a square root transformation, as indicated by a significantly lower Akaike Information Criterion compared to the Beta transformation for the final model (AIC: 182 vs. 314). We followed the same procedure for the SPC coefficient and found that a power transformation with an exponent of 0.75 was the best transformation (Supplementary Figure S5). This initial model was used for the four dependent variables:

$$study\ variable\ \sim\ Land\ use$$
$$+\ ^{15}N\ enrichment + Nitrate + Moisture + Ammonium + CO_2$$
$$+\ DOC + (1 \,|\, unique\_sample)$$

$$(7)$$

Although the ¹⁵N enrichment of the denitrifying pool appears collinear with Nitrate, these two variables represent distinct processes (correlation coefficient = - 0.29). Soil nitrate levels were measured before the incubation experiments, whereas ¹⁵N enrichment resulted from the application of ¹⁵N-labeled nitrate during the experiments. Therefore, although both variables assess the dependence of R$_{N2O}$ on nitrate, the variable Nitrate reflects the influence of native nitrate levels, while ¹⁵N enrichment captures the potential stimulation effect induced by nitrate addition. The models were then adjusted to maximize the explained variance and minimize the AIC.

The results show that CO$_2$ emissions measured from the cores were significant predictors of all four response variables. Denitrified N$_2$O emissions also depended on nitrate levels ($p < 0.1$) and moisture ($p < 0.01$) while N$_2$ emissions depended on the ¹⁵N enrichment of the soil denitrifying pool. The SPC was dependent on DOC levels ($p < 0.1$), moisture ($p < 0.001$) and ammonium ($p < 0.1$), while R$_{N2O}$ depended on nitrate levels ($p < 0.01$) and moisture ($p < 0.05$). Interestingly, neither the SPC nor R$_{N2O}$ depended on the ¹⁵N enrichment of the soil denitrifying pool. Plotting these evolutions (Figures 3a,b) confirms that the influence of the ¹⁵N enrichment on the observed values was minimal.
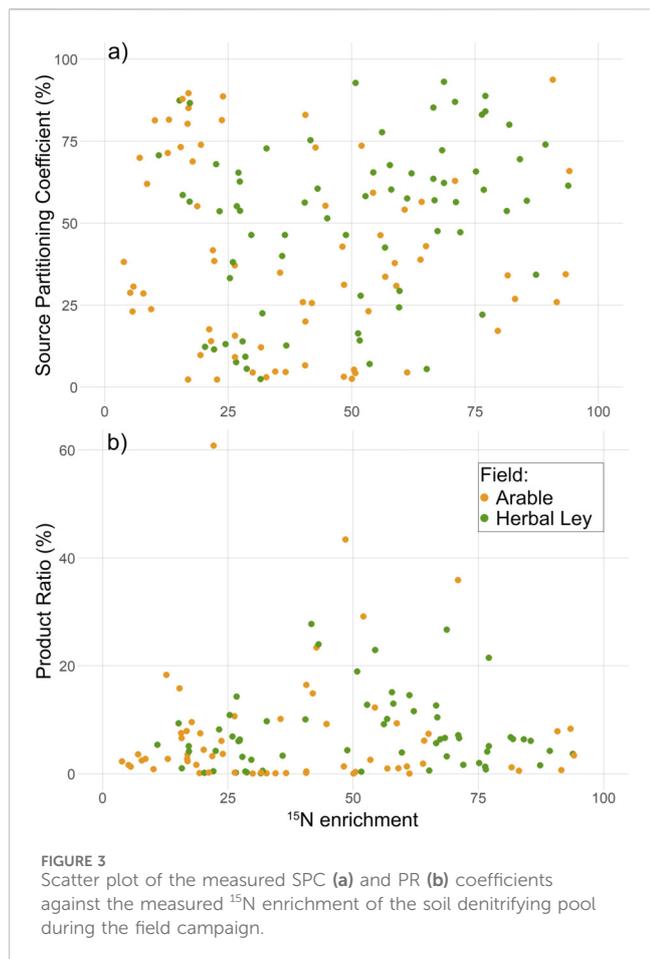
FIGURE 3
Scatter plot of the measured SPC **(a)** and PR **(b)** coefficients against the measured ^{15}N enrichment of the soil denitrifying pool during the field campaign.

3.4 Combination of liner and chamber measurements

Since the SPC and R_{N2O} were not dependent on the quantity of added tracer, we could combine liner and chamber measurements (see Section 2.5) to derive field scale fluxes of denitrification as per Equations 3, 4, (Figure 4). According to this approach, the denitrification magnitude was high in the arable field in April 2022 (~14 kg N month^{-1} ha^{-1}) following fertilizer application, although it was associated with a high uncertainty (7.4 kg N month^{-1} ha^{-1}). The rest of the time, emissions were below 3 kg N month^{-1} ha^{-1} in this field. On the other hand, the herbal ley consistently emitted denitrification fluxes below 0.2 kg N month^{-1} ha^{-1}, at the exception of April 2022, where fluxes reached 1.2 ± 0.68 kg N month^{-1} ha^{-1}. Using an initial statistical model similar as in Equation 7, denitrification fluxes were log-transformed. The final statistical model used for the total denitrification fluxes was:

$$\log(total\ denitrification) \sim Land\ use + Nitrate + Moisture + DOC + (1\,|\,unique\_sample) \tag{8}$$

In this model (R^2_m = 46%, R^2_c = 70%), Land use was the predominant fixed effect (F = 69.5, p < 0.05) while moisture played a marginal role (F = 4.12, p < 0.1). The levels of DOC were also close to a marginal effect (F = 2.47, p = 0.13).
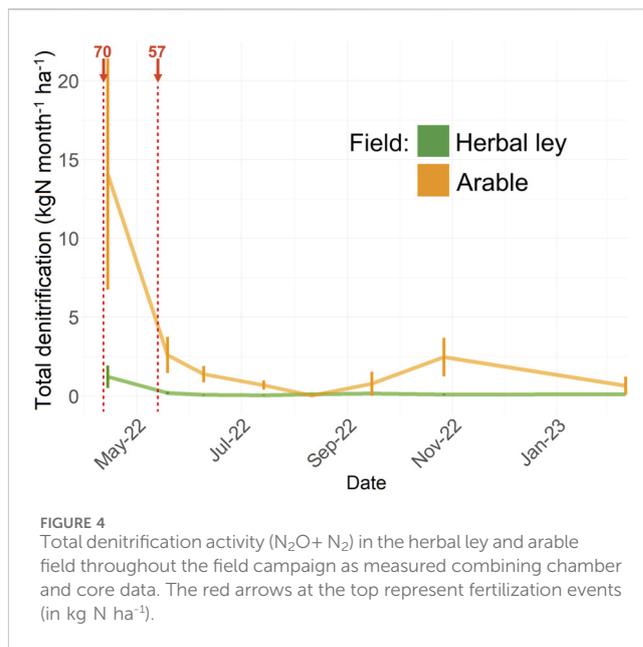

FIGURE 4
Total denitrification activity ($N_2O + N_2$) in the herbal ley and arable field throughout the field campaign as measured combining chamber and core data. The red arrows at the top represent fertilization events (in kg N ha^{-1}).

We derived an annual denitrification budget for the period from April 2022 to April 2023 to represent a full year of emission using either core measurement or the combination of core and chambers (Table 2).

The annual denitrification budgets based on either cores or cores and chambers gave similar results for the arable field, with estimated total denitrification losses of 17.97 and 22.12 kg N ha^{-1} respectively. This trend was not observed for the herbal ley where the measurements were significantly different between the two methods (14.62 and 2.41 kg N ha^{-1} respectively). Based on the core and chamber approach, and accounting for a fertilizer application rate of 179.5 kg N ha^{-1} in the arable field, we estimate a denitrification emission factor of 11% (19.71 kg N ha^{-1} losses) after subtracting background emissions measured in the herbal ley. Similarly, we can derive a N_2 emission factor of 10.2%.

4 Discussion

4.1 Application and validation of the *in situ* denitrification method

Our newly developed liner method was characterized by a high success rate of N_2 flux detection (90% of measurements). Data gaps in denitrification dataset are frequent due to the very high sensitivity required to discriminate soil-N_2 fluxes (Mulvaney and Kurtz, 1984; Kulkarni et al., 2014; Buchen et al., 2016). Although no existing number on the proportion of dataset gaps could be found, a 90% success rate can be considered very high for *in situ* denitrification measurements. Deriving a denitrification annual budget using either the core or the combination of cores and chambers results gave consistent results for the arable field, with 17.97 and 22.12 kg N ha^{-1} year^{-1} respectively (Table 1). However, this trend is not observed for the herbal ley, where the two methods yielded 14.63 and 2.41 kg N ha^{-1} year^{-1} respectively. Even when intact, soil cores do not fully reproduce field conditions, as they are laterally isolated,

TABLE 1 Results from the mixed models for denitrified N_2O, denitrified N_2, SPC and R_{N2O}. R^2m (marginal R^2) represents the variance explained by fixed effects; R^2c (conditional R^2) includes both fixed and random effects. Significant predictors (p < 0.1) are given with their significance level.

Denitrified N_2O		Denitrified N_2		SPC		R_{N2O}	
R^2_m (%)	R^2_C (%)	R^2_m (%)	R^2_C (%)	R^2_m (%)	R^2_C (%)	R^2_m (%)	R^2_C (%)
31.87	54.89	10.94	37.85	37.09	56.65	24.96	53.56
Predictor	Sign. Level	Predictor	Sign. Level	Predictor	Sign. Level	Predictor	Sign. Level
Nitrate	0.1	^{15}N enrichment	0.1	DOC	0.1	Nitrate	0.01
Moisture	0.01	CO_2	0.05	Moisture	0.001	Moisture	0.05
CO_2	0.001			Ammonium	0.1	CO_2	0.001
				CO_2	0.05		

disconnected from the surrounding soil matrix, and subject to artificial boundary conditions (liner and headspace), which can slightly reduce oxygen diffusion, facilitate gas accumulation, and stabilize anoxic microsites. Nonetheless, the observed differences between cores and chambers for the herbal ley might be better explained by a stimulation effect due to soil disturbance, release of organic carbon from the legume roots and tracer injection in the herbal ley, where consistently low nitrate levels were observed (Figure 2). In particular, the statistical analysis revealed a marginal dependence of denitrified N_2 fluxes on the ^{15}N enrichment of the nitrate pool ($p < 0.1$), reflecting a direct effect of the tracer dose applied. Another evidence for this effect is in the CO_2 fluxes, which are usually considered consistent and proportional to the amount of soil incubated (Cueva et al., 2019). Here, CO_2 fluxes followed a similar trend between cores and chambers. However, the herbal ley emitted relatively more CO_2 than the arable field in the cores compared to the chambers, resulting in a more pronounced difference between land uses under core conditions. Emissions of CO_2 were a strong indicator of denitrification activity in this study, further pointing to a stimulation effect. Although denitrification—and to some extent, nitrification—exhibits high spatial variability (Ambus and Christensen, 1993), leading to significant differences in N_2O emission magnitudes between closely located sampling points (i.e., core and chamber locations here), a stimulation effect remains the more plausible explanation here. Such effects have been previously reported in the literature (Dodds et al., 2017; Warner et al., 2019; Lewicka-Szczebak and Well, 2020).

If addition of tracer can impact the magnitude of emissions, can it influence the SPC and R_{N2O} coefficients? This was one of the key questions raised in Micucci et al. (2024), where a significant correlation between nitrate addition and R_{N2O} was observed in the laboratory but not necessarily in the field. The available literature reports several instances of product ratio stimulation under high amendment of nitrate (>75 kg N ha^{-1}; Jarvis et al., 1991; Loick et al., 2017). Here, using 144 field measurements, we show that adding tracer-level amounts of nitrate had no significant impact on these coefficients, although the p-value for the product ratio approached marginal significance ($p = 0.13$). Furthermore, field nitrate levels were a significant predictor of the R_{N2O} ($p < 0.01$), suggesting that a potential influence of the ^{15}N–NO$_3^-$ tracer cannot be completely ruled out. However, in the context of our study, there is enough

evidence to consider the R_{N2O} and SPC as independent from the addition of nitrate tracer (Figure 2) and use them in combination with N_2O fluxes measured from undisturbed soil under static chambers. The denitrification budgets for the herbal ley and arable field using this approach (2.41 and 22.12 kg N ha^{-1} year^{-1} respectively, Table 1) are much more realistic and consistent with the nitrate levels observed during the study period in these fields than the budgets derived from cores alone. Indeed, the nitrate levels were mostly below 5 kg N ha^{-1} in the herbal ley but reached almost 60 kg N ha^{-1} in the arable field (Figure 2). Therefore, the combination of core and chamber measurements was considered the most appropriate approach for estimating the denitrification budget in our study.

While the ^{15}NGF approach traces the transformation of nitrate into N_2, unlabelled ammonium can be converted to nitrate via nitrification and thereby indirectly contribute to N_2 emissions. This is relevant in the present study, as the application of ammonium and urea fertilizers (Supplementary Table S2) did not result in increased field ammonium concentrations (Figure 2), indicating that a fraction of the applied NH$_4^+$ was likely nitrified. The ^{15}NGF calculations explicitly recalculate soil ^{15}N enrichment and therefore partially account for this potential dilution of the tracer signal, although the complete nitrification-coupled pathway cannot be resolved explicitly without additional tracers.

To further improve our methodology in future studies, we suggest: i) Applying the ^{15}N tracer at the same time as the sampling of cores (i.e. 24 h before measurement), which would allow for the tracer to diffuse in the soil matrix and could potentially limit stimulation effects. In our case, the measurements were made after tracer injection to ensure sensitivity and because samplings at times 0 already shown enrichment in the ^{15}N signature of N_2O, indicating the start of tracer denitrification. However, our high success rate during this 1-year field campaign shows that sensitivity is no longer an important issue with our new method. ii) We also suggest using longer liners which will enable to sample the full soil A horizon and introduce larger headspace, where gas sampling will be less disruptive. iii) Increasing the frequency of denitrification measurements and coupling them with automated chamber and continuous analyser will allow a more thorough characterization. iv) Finally, a ^{15}N enrichment of 50% has been shown to be ideal for optimizing the sensitivity of the ^{15}N gas flux method (Micucci et al., 2023) and should be maintained as

much as possible. However, this remains particularly challenging in natural environments, where nitrate levels exhibit high spatial variability.

Overall, the combined use of core and chamber measurements aligns with recent methodologies, such as those employed by Wang et al. (2020) or Bizimana et al. (2022), where laboratory-derived product ratios were applied to field chamber data. However, in our study, the product ratio is determined under *in situ* conditions, likely providing a more accurate representation. Such an approach can help unravel the complexities of denitrification at a relatively low cost. Indeed, our method relies on the use of a small volume of artificial atmosphere to replace the headspace at the beginning of the incubation experiment and does not require a continuous flow-through system in contrast to other approaches (e.g., Cárdenas et al., 2003; Well et al., 2019a), resulting in reduced consumption of the expensive artificial atmosphere mixture. The approach nevertheless remains costly due to the use of ^{15}N tracers. Combining this method with automated flux chambers would therefore be particularly advantageous, as it would substantially increase measurement frequency—one of the main limitations of the present study—while maximizing the information gained per incubation.

4.2 Controls and dynamics of denitrification

In our study, nitrate and moisture impacted denitrified N_2O emissions, but more importantly the denitrification product ratio (Table 1), which directly affects the efficiency of denitrification as a sink for nitrous oxide. The denitrification product ratios in both fields stayed below 15% during the measurement campaign, at the exception of May 2022 where it reached 32% in the arable field. This coincides with the highest levels of nitrate recorded during our campaign (~55 kg N/ha, following fertilization, Figure 2) and with a local minimum in soil WFPS (50%). These results are consistent with the conditions that favour incomplete denitrification, such as a relatively low moisture (<75% WFPS, Davidson, 1992; Saggar et al., 2013; Weier et al., 1993) and fertilizer-levels of nitrate amendments (Clayton et al., 1997; Loick et al., 2017). Another parameter that influences denitrification is temperature, which has rarely been characterized in the field due to lack of measurements. Since denitrification is a microbially mediated process, it tends to be minimal around freezing temperatures (Dorland and Beauchamp, 1991), however the effect on the denitrification product ratio remains uncertain under field conditions. Laboratory studies have shown that increasing temperature can increase this ratio, favouring N_2O accumulation over complete reduction to N_2 (Phillips et al., 2015). Here, we characterized exceptionally low product ratios during winter, with values of 0.39% and 0.22% for the herbal ley and arable field, respectively under a temperature of 4 °C. This seems to indicate that the product ratio decreases at low temperatures, consistent with the results of Phillips et al. (2015). To our knowledge, this aspect has rarely been characterized, and more generally, the temporal variations of the product ratio under *in situ* conditions remain largely unexplored. Indeed, in a meta-analysis compiling 236 studies, it was found that 74% of the reported denitrification fluxes were measured instantaneously rather than over a time period (Almaraz et al., 2020).

Multiple microbial processes contribute to N_2O production, denitrification and nitrification are the dominant pathways (Bremner, J. M., 1997; Barnard et al., 2005; Zou et al., 2014). Therefore, the SPC essentially reflects the balance between nitrification and denitrification. In our study, it was strongly influenced ($p < 0.001$) by moisture and marginally ($p < 0.1$) by DOC content and ammonium levels. The availability of carbon substrate favors denitrification (Seitzinger et al., 2006) while ammonium promotes nitrification as it serves as its primary substrate (Ayiti and Babalola, 2022). Moisture has been shown to regulate the balance between denitrification and nitrification, in particular with a shift towards denitrification around 60%–70% WFPS (Ciarlo et al., 2007; Congreves et al., 2019; Wang et al., 2023). However, we observe an opposite trend here where the SPC is maximal during the summertime where the moisture is at a minimum. This can be explained by the very low magnitude of total N_2O fluxes during this period (<0.1 kg N ha^{-1} month^{-1} for July and August, as per measured in the static chambers), which likely makes SPC values more sensitive to small absolute variations in isotopic composition. The correlation between total denitrification and moisture ($p < 0.1$) is clearer, with higher rates in the period between April and June 2022 and in October 2023, when moisture levels were between 50% and 75% WFPS (Figure 2).

Total denitrification was mainly explained by land uses (p < 0.05), which are principally differentiated by N fertilizer application. Finally, DOC levels showed a potential influence but was not statistically significant (p = 0.13), in consistence with the controls of denitrification mentioned previously.

4.3 Annual denitrification budgets under contrasting agricultural practices

Although our annual denitrification budgets remain inherently sensitive to our sampling resolution, they show as expected that the arable field was a much bigger source of denitrified N_2O and N_2 than the herbal ley (Table 2), with a yearly loss of 22.12 kg N ha^{-1} compared to 2.41 kg N ha^{-1} (using the combination of chamber and core measurements). This loss occurred in two phases. The first phase occurred during the fertilization and growing periods (April to July 2022), with the highest fluxes recorded in April, reaching 14 kg N ha^{-1} month^{-1}. The static chambers indicated that around 2 kg N ha^{-1} month^{-1} of N_2O were lost during April and May. However, the SPC coefficient was respectively at 35% and 56%, indicating that nitrification was the dominant process in these fertilizer-derived N_2O emissions. The second phase occurred around October 2022 (~2.5 kg N ha^{-1} month^{-1}), when nitrate became available again upon rewetting. Indeed, application of fertilizer resulted in the accumulation of nitrate, which started in April 2022 (Figure 2). A large portion of this nitrate was either taken up by plants or lost to the environment by June 2022, but nitrate levels did not return to their pre-fertilization values before October. These dynamics coincided with high N fertilizer application and drought conditions (particularly in July and

TABLE 2 Mean annual denitrification measurements. The mean SPC coefficient was calculated by dividing the annual denitrified N_2O emissions by the annual total N_2O emissions. The mean R_{N2O} was calculated by dividing the annual denitrified N_2O emissions by the annual total denitrification emissions. Errors on these two coefficients were derived applying standard error propagation rules.

Approach	Field	Total N_2O (kg N ha^{-1} year^{-1})	Denitrified N_2O (kg N ha^{-1} year^{-1})	Denitrified N_2 (kg N ha^{-1} year^{-1})	Total denitrification (kg N ha^{-1} year^{-1})	Mean source partitioning coefficient (%)	Mean product ratio (%)
Cores and chambers	Herbal ley	0.34 ± 0.12	0.14 ± 0.05	2.27 ± 1.15	2.41 ± 1.20	41.18 ± 20.68	5.81 ± 3.46
	Arable	4.21 ± 1.02	1.56 ± 0.43	20.56 ± 11.20	22.12 ± 11.63	37.05 ± 13.60	7.05 ± 4.07
Cores	Herbal ley	1.35 ± 0.43	0.82 ± 0.28	13.81 ± 4.88	14.63 ± 5.16	60.74 ± 28.29	5.60 ± 2.75
	Arable	2.13 ± 0.90	0.91 ± 0.42	17.06 ± 4.10	17.97 ± 4.52	42.72 ± 26.70	5.06 ± 2.66

August, during the second most severe British drought; Barker et al., 2024), under which nitrate accumulation was observed in the soil. The return of nitrate levels to pre-fertilization levels in October coincided with milder and wetter climatic conditions following the drought and resulted in a denitrification peak of 2.5 kg N month^{-1} (Figure 4) while nitrate levels dropped by 11.2 kg N ha^{-1} (Figure 2). This nitrate build-up was also probably responsible for the high denitrification activity recorded in April/May. Under lower fertilization rates (120.5 vs. 179.5 kg N ha^{-1}) and milder climatic conditions, nitrate levels did not accumulate in 2023, likely due to more efficient plant uptake. This resulted in total N_2O emissions (as measured using static chambers) being 22 times lower. These findings suggest that denitrification was also drastically reduced in the absence of nitrate accumulation, further emphasizing the critical role of fertilizer management, including not only total nitrogen inputs but also fertilizer form and application timing. In this study, fertilizer was applied in three split applications (Supplementary Table S2); however, more refined management strategies that further synchronize nitrogen supply with crop demand may be required to limit transient nitrate accumulation and associated denitrification losses (Cassman et al., 2002). In the herbal ley, only 2.41 kg N ha^{-1} were emitted through denitrification annually, with the highest flux of 1.21 kg N ha^{-1} month^{-1} recorded in April 2022 and emissions below 0.2 kg N ha^{-1} month^{-1} the rest of the time. This is consistent with the levels of nitrate observed in this field (3 kg N ha^{-1} on average). If we assume that the difference in denitrification between the arable field and the herbal ley is primarily driven by fertilizer application, we can estimate that approximately 11% of the applied N-fertilizer was denitrified, with 7.3% of these losses being emitted as N_2O rather than N_2. This estimate remains approximate, as the herbal ley is expected to influence internal nitrogen cycling compared to an unfertilized arable field. However, given that both systems share very similar baseline soil physical and chemical properties (Supplementary Table S3)—including texture, bulk density, and pH, which strongly control oxygen diffusion, water retention, and nitrate residence time—this influence alone is unlikely to explain the large contrast in denitrification observed here. Rather, differences in fertilizer inputs and nitrate availability are expected to be the dominant drivers, suggesting that our estimates may be slightly conservative.

Overall, these results agree particularly well with the literature. Indeed, in a meta-analysis compiling 336 denitrification measurements (using chambers, cores or N balance techniques), denitrification annual budgets of agricultural soils were mostly found to be in the range of 20–30 kg N ha^{-1} year^{-1} (Hofstra and Bouwman, 2005). The results of the arable field in the present study (22.12 kg N ha^{-1} year^{-1}) are thus in good adequacy with this range. Our N_2 emission factor (10.2%) also in good agreement with the value recently reported by Kleineidam et al. (2025), who estimated it at (8.6 + 1.9) % for croplands. In their study on denitrification measurements in a German winter wheat field, Eckei et al. (2024) reported lower total denitrification losses (8.60 ± 2.21 kg N ha^{-1} over 189 days) despite a higher fertilizer application rate than in our study (210 vs. 179.5 kg N ha^{-1}). Their methodology, based on chamber-scale denitrification measurements (compared to core-scale measurements in our study), employed a more precise approach—using a continuous flush of artificial atmosphere—and more frequent measurements. This ultimately led to a more accurate quantification of denitrification. However, differences in geographic regions and management practices may also contribute to the observed discrepancies, although our results remain within the same order of magnitude. Reporting field-based experimental denitrification rates remains critical to constrain global nitrogen budgets, as denitrification is often the least quantified component—frequently missing or underestimated in global models (Bai et al., 2013).

We derived denitrification product ratios of 5.81 and 7.05 for the herbal ley and the arable field respectively (Table 1). These ratios are also in good agreement with the literature. In a meta-analysis on terrestrial denitrification N fluxes, Scheer et al. (2020) reported a mean denitrification product ratio of 8% (6%–11%); and more specifically a ratio of (12.40 ± 3.1) % for soils under natural vegetation and (10.90 ± 2.0) % for agricultural soils. More recently, Kleineidam et al. (2025) compiled 18 studies and found mean product ratios of 12% for grassland and 16% for croplands (and medians of 4% and 8% respectively). Eckei et al. (2024), who also followed temporal dynamics of denitrification (although not in winter) found 12% in the German winter wheat crop amended with 210 kg N ha^{-1} of fertilizer. Our results are thus in the lower range of the reported values. This could potentially be explained by the slightly alkaline pH of the FarmED soil (Supplementary Table S3), which tends to favour the reduction of N_2O to N_2, thereby decreasing the denitrification product ratio (ŠImek and Cooper,

2002). Furthermore, if we look at monthly reported values (Figure 1), product ratios around 10% are frequently encountered (especially between June and August). If most of the studies analysed by Kleineidam et al. (2025) and Scheer et al. (2020) measured this ratio in one-time experiments—as was the case in 74% of studies according to Almaraz et al. (2020)—this could explain why our annual mean ratios are slightly lower than the reported values.

5 Conclusion

The combination of the ^{15}N Gas Flux method with an artificial atmosphere represents a powerful tool to constrain denitrification. Our new denitrification measurement approach proved to be both cost-effective and promising in helping to unravel the complexities of the denitrification process. The resulting denitrification budgets reveal that ineffective fertilizer uptake leads to nitrogen accumulation, which can amplify denitrification during future applications, increase the $N_2O/(N_2O + N_2)$ ratio, and reduce the system's ability to act as a nitrous oxide sink. A higher measurement frequency coupled with continuous chamber-based measurements will enable a better characterization of denitrification dynamics, including total fluxes, product ratios, N_2O source partitioning and spatio-temporal variations, to help improve N management in agricultural ecosystems.

Data availability statement

The datasets presented in this study can be found in online repositories. The names of the repository/repositories and accession number(s) can be found below: https://data.mendeley.com/datasets/zwkhfxscjz/1.

Author contributions

GM: Conceptualization, Data curation, Formal Analysis, Funding acquisition, Investigation, Methodology, Resources, Validation, Visualization, Writing – original draft, Writing – review and editing. FS: Conceptualization, Formal Analysis, Investigation, Resources, Supervision, Writing – original draft, Writing – review and editing. JL: Project administration, Resources, Supervision, Validation, Writing – original draft, Writing – review and editing. SU: Funding acquisition, Investigation, Methodology, Project administration, Resources, Supervision, Writing – original draft, Writing – review and editing.

Funding

Acknowledgements

Conflict of interest

The author(s) declared that this work was conducted in the absence of any commercial or financial relationships that could be construed as a potential conflict of interest.

Generative AI statement

The author(s) declared that generative AI was used in the creation of this manuscript. Generative AI was used occasionally to revise, edit, and polish the English language of the manuscript. The AI was not used to generate scientific content, and all AI-assisted edits were checked by the authors for accuracy and correctness.

Any alternative text (alt text) provided alongside figures in this article has been generated by Frontiers with the support of artificial intelligence and reasonable efforts have been made to ensure accuracy, including review by the authors wherever possible. If you identify any issues, please contact us.

Publisher's note

All claims expressed in this article are solely those of the authors and do not necessarily represent those of their affiliated organizations, or those of the publisher, the editors and the reviewers. Any product that may be evaluated in this article, or claim that may be made by its manufacturer, is not guaranteed or endorsed by the publisher.

Supplementary material

The Supplementary Material for this article can be found online at: https://www.frontiersin.org/articles/10.3389/fenvs.2026.1750986/full#supplementary-material

References

Almaraz, M., Wong, M. Y., and Yang, W. H. (2020). Looking back to look ahead: a vision for soil denitrification research. *Ecology* 101, e02917. doi:10.1002/ecy.2917

Ambus, P., and Christensen, S. (1993). Denitrification variability and control in a riparian fen irrigated with agricultural drainage water. *Soil Biol. biochem.* 25, 915–923. doi:10.1016/0038-0717(93)90094-R

Anthony, W. H., Hutchinson, G. L., and Livingston, G. P. (1995). Chamber measurement of soil-atmosphere gas exchange: Linear vs. diffusion-based flux models. *Soil Sci. Soc. Am. J.* 59, 1308–1310. doi:10.2136/sssaj1995.03615995005900050015x

Ayiti, O. E., and Babalola, O. O. (2022). Factors influencing soil nitrification process and the effect on environment and health. *Front. Sustain. Food Syst.* 6, 821994. doi:10.3389/fsufs.2022.821994

Bai, E., Li, S., Xu, W., Li, W., Dai, W., and Jiang, P. (2013). A meta-analysis of experimental warming effects on terrestrial nitrogen pools and dynamics. *New Phytol.* 199, 441–451. doi:10.1111/nph.12252

Barker, L. J., Hannaford, J., Magee, E., Turner, S., Sefton, C., Parry, S., et al. (2024). An appraisal of the severity of the 2022 drought and its impacts. *Weather* 79, 208–219. doi:10.1002/wea.4531

Barnard, R., Leadley, P. W., and Hungate, B. A. (2005). Global change, nitrification, and denitrification: a review. *Glob. Biogeochem. Cycles* 19, 2004GB002282. doi:10.1029/2004GB002282

Biswas, B., and Gresshoff, P. M. (2014). The role of symbiotic nitrogen fixation in sustainable production of biofuels. *Int. J. Mol. Sci.* 15, 7380–7397. doi:10.3390/ijms15057380

Bizimana, F., Luo, J., Timilsina, A., Dong, W., Gaudel, G., Ding, K., et al. (2022). Estimating field N2 emissions based on laboratory-quantified N2O/(N2O + N2) ratios and field-quantified N2O emissions. *J. Soils Sediments* 22, 2196–2208. doi:10.1007/s11368-022-03212-0

Bremner, J. M. (1997). "Sources of nitrous oxide in soils,", 49. Kluwer Academic Publishers, 7–16. doi:10.1023/a:1009798022569

Buchen, C., Lewicka-Szczebak, D., Fuß, R., Helfrich, M., Flessa, H., and Well, R. (2016). Fluxes of N2 and N2O and contributing processes in summer after grassland renewal and grassland conversion to maize cropping on a plaggic anthrosol and a histic gleysol. *Soil Biol. biochem.* 101, 6–19. doi:10.1016/j.soilbio.2016.06.028

Cárdenas, L. M., Hawkins, J. M. B., Chadwick, D., and Scholefield, D. (2003). Biogenic gas emissions from soils measured using a new automated laboratory incubation system. *Soil Biol. biochem.* 35, 867–870. doi:10.1016/S0038-0717(03)00092-0

Cassman, K. G., Dobermann, A., and Walters, D. T. (2002). Agroecosystems, nitrogen-use efficiency, and nitrogen management. *AMBIO J. Hum. Environ.* 31, 132–140. doi:10.1579/0044-7447-31.2.132

Ciarlo, E., Conti, M., Bartoloni, N., and Rubio, G. (2007). The effect of moisture on nitrous oxide emissions from soil and the N2O/(N2O+N2) ratio under laboratory conditions. *Biol. Fertil. Soils* 43, 675–681. doi:10.1007/s00374-006-0147-9

Clayton, H., McTaggart, I. P., Parker, J., Swan, L., and Smith, K. A. (1997). Nitrous oxide emissions from fertilised grassland: a 2-year study of the effects of N fertiliser form and environmental conditions. *Biol. Fertil. Soils* 25, 252–260. doi:10.1007/s003740050311

Congreves, K. A., Phan, T., and Farrell, R. E. (2019). A new look at an old concept: using[15] N2 O isotopomers to understand the relationship between soil moisture and N2 O production pathways. *SOIL* 5, 265–274. doi:10.5194/soil-5-265-2019

Conthe, M., Lycus, P., Arntzen, M. Ø., Ramos da Silva, A., Frostegård, Å., Bakken, L. R., et al. (2019). Denitrification as an N2O sink. *Water Res.* 151, 381–387. doi:10.1016/j.watres.2018.11.087

Cueva, A., Volkmann, T. H. M., Van Haren, J., Troch, P. A., and Meredith, L. K. (2019). Reconciling negative soil CO2 fluxes: insights from a large-scale experimental hillslope. *Soil Syst.* 3, 10. doi:10.3390/soilsystems3010010

Davidson, E. A. (1992). Sources of nitric oxide and nitrous oxide following wetting of dry soil. *Soil Sci. Soc. Am. J.* 56, 95–102. doi:10.2136/sssaj1992.03615995005600010015x

Dodds, W. K., Burgin, A. J., Marcarelli, A. M., and Strauss, E. A. (2017). "Nitrogen transformations," in *Methods in stream ecology*. Third Edition (Elsevier), 173–196. doi:10.1016/B978-0-12-813047-6.00010-3

Dorland, S., and Beauchamp, E. G. (1991). Denitrification and ammonification at low soil temperatures. *Can. J. Soil Sci.* 71, 293–303. doi:10.4141/cjss91-029

Eckei, J., Well, R., Maier, M., Matson, A., Dittert, K., and Rummel, P. S. (2024). Determining N2O and N2 fluxes in relation to winter wheat and sugar beet growth and development using the improved 15N gas flux method on the field scale. *Biol. Fertil. Soils.* 61, 489–505. doi:10.1007/s00374-024-01806-z

FAO - Food and Agriculture Organization of the United Nations (2017). World fertilizer trends and outlook to 2020. Available online at: https://www.fao.org/3/i6895e/i6895e.pdf.

Friedl, J., Cardenas, L. M., Clough, T. J., Dannenmann, M., Hu, C., and Scheer, C. (2020). Measuring denitrification and the N2O:(N2O + N2) emission ratio from terrestrial soils. *Curr. Opin. Environ. Sustain.* 47, 61–71. doi:10.1016/j.cosust.2020.08.006

Groffman, P. M., Altabet, M. A., Böhlke, J. K., Butterbach-Bahl, K., David, M. B., Firestone, M. K., et al. (2006). Methods for measuring denitrification: diverse approaches to a difficult problem. *Ecol. Appl.* 16, 2091–2122. doi:10.1890/1051-0761(2006)016%5B2091:MFMDDA%5D2.0.CO;2

Groffman, P. M., Butterbach-Bahl, K., Fulweiler, R. W., Gold, A. J., Morse, J. L., Stander, E. K., et al. (2009). Challenges to incorporating spatially and temporally explicit phenomena (hotspots and hot moments) in denitrification models. *Biogeochemistry* 93, 49–77. doi:10.1007/s10533-008-9277-5

Hofstra, N., and Bouwman, A. F. (2005). Denitrification in agricultural soils: summarizing published data and estimating global annual rates. *Nutr. Cycl. Agroecosyst.* 72, 267–278. doi:10.1007/s10705-005-3109-y

Hutchinson, G. L., and Mosier, A. R. (1981). Improved soil cover method for field measurement of nitrous oxide fluxes. *Soil Sci. Soc. Am. J.* 45, 311–316. doi:10.2136/sssaj1981.03615995004500020017x

IPCC (Intergovernmental Panel On Climate Change) (2023). *Climate change 2021 – the Physical Science Basis: Working Group I contribution to the sixth assessment report of the intergovernmental Panel on climate change.* 1st Edn. Cambridge University Press. doi:10.1017/9781009157896

Jarvis, S. C., Barraclough, D., Williams, J., and Rook, A. J. (1991). Patterns of denitrification loss from grazed grassland: effects of N fertilizer inputs at different sites. *Plant Soil* 131, 77–88. doi:10.1007/BF00010422

Jordon, M. W., Willis, K. J., Bürkner, P.-C., and Petrokofsky, G. (2022). Rotational grazing and multispecies herbal leys increase productivity in temperate pastoral systems – a meta-analysis. *Agric. Ecosyst. Environ.* 337, 108075. doi:10.1016/j.agee.2022.108075

Kleineidam, K., Böttcher, J., Butterbach-Bahl, K., Dannenmann, M., Dittert, K., Dörsch, P., et al. (2025). Denitrification in agricultural Soils – integrated control and Modelling at various scales (DASIM). *Biol. Fertil. Soils.* doi:10.1007/s00374-025-01894-5

Kulkarni, M. V., Burgin, A. J., Groffman, P. M., and Yavitt, J. B. (2014). Direct flux and 15N tracer methods for measuring denitrification in forest soils. *Biogeochemistry* 117, 359–373. doi:10.1007/s10533-013-9876-7

Lassaletta, L., Billen, G., Grizzetti, B., Anglade, J., and Garnier, J. (2014). 50 year trends in nitrogen use efficiency of world cropping systems: the relationship between yield and nitrogen input to cropland. *Environ. Res. Lett.* 9, 105011. doi:10.1088/1748-9326/9/10/105011

Laughlin, R. J., Stevens, R. J., Laughlin, R. J., and Stevens, R. J. (2002). Evidence for fungal Dominance of Denitrification and Codenitrification in a Grassland Soil optimal soil moisture content, glucose con-centration, and inhibitor concentrations were determined in.

Lewicka-Szczebak, D., and Well, R. (2020). The 15N gas-flux method to determine N2 flux: a comparison of different tracer addition approaches. *SOIL* 6, 145–152. doi:10.5194/soil-6-145-2020

Loick, N., Dixon, E., Abalos, D., Vallejo, A., Matthews, P., McGeough, K., et al. (2017). "Hot spots" of N and C impact nitric oxide, nitrous oxide and nitrogen gas emissions from a UK grassland soil. *Geoderma* 305, 336–345. doi:10.1016/j.geoderma.2017.06.007

Matsuoka, M., Kumar, A., Muddassar, M., Matsuyama, A., Yoshida, M., and Zhang, K. Y. J. (2017). Discovery of fungal denitrification inhibitors by targeting copper nitrite reductase from Fusarium oxysporum. *J. Chem. Inf. Model.* 57, 203–213. doi:10.1021/acs.jcim.6b00649

Meng, P., Pei, H., Hu, W., Shao, Y., and Li, Z. (2014). How to increase microbial degradation in constructed wetlands: influencing factors and improvement measures. *Bioresour. Technol.* 157, 316–326. doi:10.1016/j.biortech.2014.01.095

Micucci, G., Sgouridis, F., McNamara, N. P., Krause, S., Lynch, I., Roos, F., et al. (2023). The 15N-Gas flux method for quantifying denitrification in soil: current progress and future directions. *Soil Biol. Biochem.* 184, 109108. doi:10.1016/j.soilbio.2023.109108

Micucci, G., Sgouridis, F., McNamara, N. P., Krause, S., Lynch, I., Roos, F., et al. (2024). Towards enhanced sensitivity of the 15N gas flux method for quantifying denitrification in soil. *Soil Biol. biochem.* 194, 109421. doi:10.1016/j.soilbio.2024.109421

Micucci, G., Lewicka-Szczebak, D., Sgouridis, F., Well, R., Buchen-Tschiskale, C., McNamara, N. P., et al. (2025). Combining the[15] N gas flux method and N2 O isotopocule data for the determination of soil microbial N2 O sources. *Rapid Commun. Mass Spectrom.* 39 (6), e9971. doi:10.1002/rcm.9971

Miller-Klugesherz, J. A., and Sanderson, M. R. (2023). Good for the soil, but good for the farmer? Addiction and recovery in transitions to regenerative agriculture. *J. Rural. Stud.* 103, 103123. doi:10.1016/j.jrurstud.2023.103123

Mulvaney, R. L., and Kurtz, L. T. (1984). Evolution of dinitrogen and nitrous oxide from Nitrogen-15 fertilized soil cores subjected to wetting and drying cycles. *Soil Sci. Soc. Am. J.* 48, 596–602. doi:10.2136/sssaj1984.03615995004800030026x

Munch, J. C., and Velthof, G. L. (2007). "Denitrification and agriculture," in *Biology of the nitrogen cycle* (Elsevier), 331–341. doi:10.1016/B978-044452857-5.50022-9

Overton, M. (1996). Re-establishing the english agricultural revolution. *Agric. Hist. Rev.* 44, 1–20.

Pedersen, A. R., Petersen, S. O., and Schelde, K. (2010). A comprehensive approach to soil-atmosphere trace-gas flux estimation with static chambers. *Eur. J. Soil Sci.* 61, 888–902. doi:10.1111/j.1365-2389.2010.01291.x

Phillips, R., McMillan, A., Palmada, T., Dando, J., and Giltrap, D. (2015). Temperature effects on N_2O and N_2 denitrification end-products for a New Zealand pasture soil. *N. Z. J. Agric. Res.* 58, 89–95. doi:10.1080/00288233.2014.969380

Ravishankara, A. R., Daniel, J. S., and Portmann, R. W. (2009). Nitrous oxide (N2O): the dominant ozone-depleting substance emitted in the 21st century. *Science* 326, 123–125. doi:10.1126/science.1176985

Rockström, J., Gupta, J., Qin, D., Lade, S. J., Abrams, J. F., Andersen, L. S., et al. (2023). Safe and just Earth system boundaries. *Nature* 619, 102–111. doi:10.1038/s41586-023-06083-8

Saggar, S., Jha, N., Deslippe, J., Bolan, N. S., Luo, J., Giltrap, D. L., et al. (2013). Denitrification and N2O:N2 production in temperate grasslands: processes, measurements, modelling and mitigating negative impacts. *Sci. Total Environ.* 465, 173–195. doi:10.1016/j.scitotenv.2012.11.050

Scheer, C., Fuchs, K., Pelster, D. E., and Butterbach-bahl, K. (2020). ScienceDirect estimating global terrestrial denitrification from measured N 2 O:(N 2 O + N 2) product ratios. *Curr. Opin. Environ. Sustain.* 47, 72–80. doi:10.1016/j.cosust.2020.07.005

Seitzinger, S., Harrison, J. A., Böhlke, J. K., Bouwman, A. F., Lowrance, R., Peterson, B., et al. (2006). Denitrification across landscapes and waterscapes: a synthesis. *Ecol. Appl.* 16, 2064–2090. doi:10.1890/1051-0761(2006)016%5B2064:DALAWA%5D2.0.CO;2

Šimek, M., and Cooper, J. E. (2002). The influence of soil pH on denitrification: progress towards the understanding of this interaction over the last 50 years. *Eur. J. Soil Sci.* 53, 345–354. doi:10.1046/j.1365-2389.2002.00461.x

Soana, E., Vincenzi, F., Colombani, N., Mastrocicco, M., Fano, E. A., and Castaldelli, G. (2022). Soil denitrification, the missing piece in the puzzle of nitrogen budget in lowland agricultural basins. *Ecosystems* 25, 633–647. doi:10.1007/s10021-021-00676-y

Wang, R., Pan, Z., Zheng, X., Ju, X., Yao, Z., Butterbach-Bahl, K., et al. (2020). Using field-measured soil N2O fluxes and laboratory scale parameterization of N2O/(N2O+N2) ratios to quantify field-scale soil N2 emissions. *Soil Biol. biochem.* 148, 107904. doi:10.1016/j.soilbio.2020.107904

Wang, H., Yan, Z., Ju, X., Song, X., Zhang, J., Li, S., et al. (2023). Quantifying nitrous oxide production rates from nitrification and denitrification under various moisture conditions in agricultural soils: laboratory study and literature synthesis. *Front. Microbiol.* 13, 1110151. doi:10.3389/fmicb.2022.1110151

Warner, D. I., Scheer, C., Friedl, J., Rowlings, D. W., Brunk, C., and Grace, P. R. (2019). Mobile continuous-flow isotope-ratio mass spectrometer system for automated measurements of N2O fluxes in fertilized cropping systems. *Sci. Rep.* 9, 11097. doi:10.1038/s41598-019-47451-7

Weier, K. L., Doran, J. W., Power, J. F., and Walters, D. T. (1993). Denitrification and the Dinitrogen/Nitrous oxide ratio as affected by soil water, available carbon, and nitrate. *Soil Sci. Soc. Am. J.* 57, 66–72. doi:10.2136/sssaj1993.03615995005700010013x

Well, R., Burkart, S., Giesemann, A., Grosz, B., Köster, J. R., and Lewicka-Szczebak, D. (2019a). Improvement of the [15] N gas flux method for *in situ* measurement of soil denitrification and its product stoichiometry. *Rapid Commun. Mass Spectrom.* 33, 437–448. doi:10.1002/rcm.8363

Well, R., Maier, M., Lewicka-Szczebak, D., Köster, J. R., and Ruoss, N. (2019b). Underestimation of denitrification rates from field application of the 15N gas flux method and its correction by gas diffusion modelling. *Biogeosciences* 16, 2233–2246. doi:10.5194/bg-16-2233-2019

Zaman, M., Heng, L., and Müller, C. (2021). Measuring emission of agricultural greenhouse gases and developing mitigation options using nuclear and related techniques: applications of nuclear techniques for GHGs. *App. Nuclear Tech.* 337. doi:10.1007/978-3-030-55396-8

Zou, Y., Hirono, Y., Yanai, Y., Hattori, S., Toyoda, S., and Yoshida, N. (2014). Isotopomer analysis of nitrous oxide accumulated in soil cultivated with tea (Camellia sinensis) in Shizuoka, central Japan. *Soil Biol. biochem.* 77, 276–291. doi:10.1016/j.soilbio.2014.06.016